The Local Hubble Flow: Is it a Manifestation of Dark Energy?

Yehuda Hoffman[1], Luis A. Martinez-Vaquero[2], Gustavo Yepes[2] and Stefan Gottlöber[3]

[1] *Racah Institute of Physics, Hebrew University, Jerusalem 91904, Israel*
[2] *Grupo de Astrofísica, Universidad Autónoma de Madrid, Madrid E-28049, Spain*
[3] *Astrophysikalisches Institut Potsdam, An der Sternwarte 16, 14482 Potsdam, Germany*

25 October 2018

ABSTRACT
To study the local Hubble flow, we have run constrained dark matter (DM) simulations of the Local Group (LG) in the concordance ΛCDM and OCDM cosmologies, with identical cosmological parameters apart from the Λ term. The simulations were performed within a computational box of $64\,h^{-1}$Mpc centred on the LG. The initial conditions were constrained by the observed peculiar velocities of galaxies and positions of X-ray nearby clusters of galaxies. The simulations faithfully reproduce the nearby large scale structure, and in particular the Local Supercluster and the Virgo cluster. LG-like objects have been selected from the DM halos so as to closely resemble the dynamical properties of the LG. Both the ΛCDM and OCDM simulations show very similar local Hubble flow around the LG-like objects. It follows that, contrary to recent statements, the dark energy (DE) does not manifest itself in the local dynamics.

Key words: galaxies: Local Group – cosmology: dark matter – methods: N-body simulations

1 INTRODUCTION

It has been recently stated that the cosmological constant (Λ) or its generalisation the dark energy (DE), manifests itself in the dynamics of the local universe (Baryshev et al. 2001, Chernin et al. 2004, Teerikorpi et al. 2005, Chernin et al. 2006, Chernin et al. 2007b, and Chernin et al. 2007c). In these papers, the coldness of the local Hubble flow around the Local Group (LG) has been attributed to the existence DE. This has been supported by Macciò et al. (2005) who analysed a set of N-body simulations and concluded that indeed *...[their] results provide new, independent evidence for the presence of dark energy on scales of a few megaparsecs*. These results, if correct, would have provided an independent corroboration to the DE component whose existence is otherwise inferred from observations of distant objects and the early Universe. These authors used the term 'local' as describing the neighborhood of the LG out to a distance of a few Mpc.

Much of the dynamical implications of the cosmological constant for the large scale structure were worked out by Lahav et al. (1991). The LG constitutes a quasi-linear object and therefore its dynamics cannot be modeled by the linear theory or the spherical top-hat model. Consequently, we have recently studied the local universe

by means of constrained simulations (CSs, Kravtsov et al. 2002, Klypin et al. 2003, Martinez-Vaquero et al. 2007 and Hoffman et al. 2007). The unique feature of the CSs is that their initial conditions are generated as constrained realizations of Gaussian random fields (Hoffman & Ribak 1991). The initial conditions are constrained by observational data and hence they are designed to reproduce the main gross features of the local large scale structure. As such they provide the optimal tool for studying the dynamics of the LG, being a given individual but not an atypical object. In particular the recent constrained flat Λ dominated (ΛCDM) and open (OCDM) cold dark matter N-body simulations of Martinez-Vaquero et al. (2007) were designed to study the local dynamics in cold dark matter cosmologies with and without a DE component. These simulations are to be used here as a laboratory for thesting the hypothesis that the cold local Hubble flow is a signature of dark energy. We are less interested here in the actual coldness of the flow and more in the possibility that the DE affects the local flow. A thorough analysis of the issue of the coldness of the local flow is to be given elsewhere (Martinez-Vaquero et al, in preparation). In what follows 'local' is defined as the region contained in a sphere of radius $R = 3$ Mpc centred on the LG.

The structure of the paper is as follows. A very brief review of the simulations of Martinez-Vaquero et al. (2007)

is presented in Section 2. The selection criteria for LG candidates are summarised in Section 3. The flow fields around the simulated LG candidates in the ΛCDM and OCDM simulations are presented in Section 4. In Section 5 we compare the gravitational field around the LG candidates. A general discussion concludes the paper (Section 6).

2 CONSTRAINED SIMULATIONS OF THE LOCAL UNIVERSE

Our CSs have already been used in Martinez-Vaquero et al. (2007) and they are briefly summarised here. These are dark matter (DM) only simulations employing a periodic cubic computational box of $64\,h^{-1}$Mpc on a side using 256^3 particles. Both models use the dimensionless Hubble constant of $h = 0.7$ (where $h = H_0/100$ km/s/Mpc), the power spectrum normalisation $\sigma_8 = 0.9$ and the cosmological matter density of $\Omega_m = 0.3$. The ΛCDM model corresponds to a flat universe with $\Omega_\Lambda = 1 - \Omega_m$ while for the OCDM model $\Omega_\Lambda = 0$. These cosmological parameters correspond to the so-called Concordance Model. We used the parallel TREEPM N-body code GADGET2 (Springel, 2005) to run these simulations. For the PM part of the algorithm, we used a uniform grid of 512^3 mesh points to estimate the long-range gravitational force by means of FFT techniques. The gravitational smoothing used to compute the short-scale gravitational forces correspond to an equivalent Plummer smoothing parameter of $\epsilon = 15h^{-1}$ kpc comoving.

The number of particles used in these simulations (256^3) provides a very mild mass resolution ($1.3 \times 10^9\,h^{-1}\mathrm{M}_\odot$ per particle) which corresponds to a minimal mass of the DM halos of $\approx 2.5 \times 10^{10}\,h^{-1}\mathrm{M}_\odot$, for objects resolved with more than 20 dark matter particles. At such a resolution the inner structure of the main halos of the LG-like objects cannot be resolved, nor can the observed mass distribution of the LG nearby dwarfs be reconstructed. Yet, the dynamics on the scale of a very few Mpc is very well resolved.

We set up initial conditions for these simulations in such a way that we can zoom in to any particular object with much more resolution. Thus, we generate the random realizations of the density fluctuation field for a much larger number of particles (up to 4096^3). Then, we substitute the fourier modes corresponding to the small wavenumber by those coming from the constrained 256^3 density field and make the displacement fields according to the Zeldovich approximation. Thus, we can now resimulate any particular zone of the simulated volume with particles of variable masses, down to 4096 times smaller than the particle mass of the simulations used in this work. A comparison of the results of ΛCDM 256^3 simulation with that from the LG-like systems resimulated at 4096^3 resolution does not yield any significant differences in their Hubble diagrams (to be published).

The algorithm of constrained realizations of Gaussian random fields (Hoffman & Ribak, 1991) has been used to set up the initial conditions. The data used to constrain the initial conditions of the simulations is made of two kinds. The first data set is made of radial velocities of galaxies drawn from the MARK III (Willick et al. 1997), SBF (Tonry et al. 2001) and the Karachentsev (2005) catalogues. Peculiar velocities are less affected by non-linear effects and are used

as constraints as if they were linear quantities (Zaroubi, Hoffman & Dekel 1999). This follows the CSs performed by Kravtsov et al. (2002) and Klypin et al. (2003). The other constraints are obtained from the catalog of nearby X-ray selected clusters of galaxies (Reiprich & Böhringer 2002). Given the virial parameters of a cluster and assuming the spherical top-hat model one can derive the linear overdensity of the cluster. The large scale structure, *i.e.* scales somewhat larger than $5\,h^{-1}$Mpc, of the resulting density and velocity fields are strongly constrained by the imposed data. In particular all the resulting CSs are dominated by a Local Supercluster (LSC) - like object with a Virgo size DM halo at its center. The LG is not directly imposed on the initial conditions, but having reconstructed the actual large scale structure of the local universe a LG-like structure is very likely to emerge in the right place with dynamical properties similar to the actual ones. The two simulations used here are based on the same random realization of the initial conditions.

3 SELECTION OF LG-LIKE CANDIDATES

The selection of LG candidates is described in detail in Martinez-Vaquero et al. (2007). The selection of the objects is based on the Macciò et al. (2005) criteria, which consist of:

i. The group contains two MW and M31 like DM halos with maximum circular velocity in the range of $125 \leqslant V_c \leqslant 270$ km/s.

ii. The two major DM halos are separated by no more than $1\,h^{-1}$Mpc.

iii. The relative radial velocity of the two main halos is negative.

iv. There are no objects with maximum circular velocity higher than MW and M31 candidates within a distance of $3\,h^{-1}$Mpc.

v. The group resides within a distance of 5 to $12\,h^{-1}$Mpc from a Virgo like halo of $500 \leqslant V_c \leqslant 1500$ km/s.

DM halos are found using both the Bound Density Maxima algorithm (Klypin et al., 1999) and the AMIGA Halo Finder (Gill et al., 2004). In the ΛCDM simulation 26 LG-like objects have been found and 43 in the OCDM one. Given the fact that both simulation are based on the same realization of the random Gaussian field we have identified 9 LG-like objects that appear in both simulations at about the same position and are very similar dynamically. We refer to these as the 'same' objects appearing in both simulations. These 'same' objects do not form any class by themselves and are statistically indistinguishable from the other LG-like objects. These objects are used here to exemplify the effect of the Λ term on the dynamics of the LG, as they are the *same* object evolving in two identical cosmologies and environments that differ only by their Λ term.

The fact that there is no one-to-one coincidence of the LG-like objects of the two simulations should not be surprising. There are two reasons for that. First, the two cosmologies are not identical and they differ in the linear gravitational growth function. Second, the LG is a system in the quasi-linear regime and is far from being in dynamical equilibrium. Had we observed it at a slightly different time it

might not be qualified as a LG-like object according to the selection criteria assumed here. This is certainly the case for our simulated objects. Just a small miss match in the dynamical phase of the objects between the two simulations can rule out an object in one or the other simulation from being a LG-like systems.

In the present paper we are interested in comparing the local Hubble flow around LG-like objects. Providing that the selected systems fulfil all requirements their exact location is not important for the purpose of the analysis.. Therefore, we have used all the objects found within the computational box, regardless of their position with respect to the LSC. Some simulated LG-like objects reside close to the actual position of the LG but they seem to be dynamically indistinguishable from the others.

4 THE LOCAL HUBBLE FLOW

The local Hubble flow around LG-like objects is probed by means of Hubble diagrams showing the radial velocities relative to the objects center of mass within a distance of 3 Mpc. In Figs. 1 and 2 we present the Hubble diagrams of 4 randomly chosen candidates out of the 9 LG-like objects which appear in both simulations (Fig. 1: ΛCDM, Fig. 2: OCDM). The figures present all the DM halos around the chosen LG-like objects out to a distance of 3 Mpc. A careful comparison of the plots reveals that the Hubble diagrams of a given ΛCDM and OCDM simulated LG are very similar. In particular the *r.m.s.* value of the scatter around a pure Hubble flow (σ_H, assuming the true value of the Hubble constant of the simulation) does not vary statistically between the ΛCDM and OCDM cases. For the 4 objects shown in Figs 1 and 2, we find $\sigma_H = 35$, 38, 42 and 53 km/s for the ΛCDM objects and 41, 42, 55 and 59 km/s in the OCDM case. The values of σ_H for the other 5 common candidates are 31, 51, 11, 41 and 79 km/s for the objects in the ΛCDM simulation and 61, 38, 18, 63 and 48 km/s in the OCDM one.

Much of the theoretical expectations for the possible manifestation of the DE in the local flow is based on the model proposed by Chernin et al. (2007c, and references therein). The model essentially assumes that the local gravity field around the LG can be decomposed into the contribution of the LG, modeled as a point particle, and the contribution of the DE:

$$g_{PP}(r) = -\frac{GM_{LG}}{r^2} + \Omega_\Lambda H_0^2 r \qquad (1)$$

The zero gravity surface is defined by $g_{PP}(R_V) = 0$. The radius of the zero gravity surface, R_V, plays a critical role in that simple model. A central prediction of the model is that the local Hubble flow should not contain galaxies with radial velocities smaller than the escape velocity (see the Appendix), calculated under the assumption that the gravitational field is given by the point particle approximation (Chernin et al. 2007b). This prediction excludes galaxies residing within the LG itself, namely within 0.7 Mpc. To test the prediction the radial escape velocity profiles (Eq. 6) have been plotted in both Figs. 1 and 2 as solid (ΛCDM model) and dashed (OCDM model) lines. From here on the term 'escape velocity' refers to the one calculated under the assumption of the point particle approximation.

r (Mpc)	Obs.	ΛCDM	OCDM
[0.75 − 2]	65	63	62
[0.75 − 3]	68	72	75

Table 1. The value of σ_H (in units of km/s) of the LG, compiled from the Karachentsev data, and of the ΛCDM and OCDM LG-like objects combined together, in the manner of Fig. 3. Two distance cuts are used for calculating σ_H.

Inspection of the ΛCDM Hubble diagram (Fig. 1) shows that indeed the prediction of Chernin et al. (2007b) is confirmed: only two LG-like groups have, within the range $(0.7 − 3)$ Mpc, a very few halos each with a peculiar velocity smaller than the ΛCDM escape velocity. However, this behaviour is reproduced by the OCDM LG-like objects equally well (Fig. 2).

To increase the statistical significance of the Hubble diagram analysis we have considered all the LG-like objects in the ΛCDM and OCDM simulations. This is performed by plotting the radial velocities of all halos near the LG-like groups against their distance r. Again, the Hubble diagram of all LG-like objects in both cosmologies looks very similar. In fact, the fraction of halos below the escape velocity is somewhat smaller in the OCDM objects than in the ΛCDM ones. We conclude that the ΛCDM escape velocity prediction is reproduced by the OCDM simulation.

The paper focuses mainly on the possible role of the DE in the dynamics of the LG. A thorough analysis of the coldness of the local flow will be given elsewhere (Martinez-Vaquero et al, in preparation). Here a very brief summary of the subject is given. The very local Hubble flow has been recently studied by Karachentsev et al. (2007) and their currently updated catalog of local peculiar velocities has been analyzed here (I. Karachentsev, private communication). Table I presents the value of σ_H taken over all the DM halos (simulations) or galaxies (data) in the range of $[0.75 − 2]$ Mpc and $[0.75 − 3]$ Mpc of the Karachentsev's data and of the ΛCDM and the OCDM LG-like objects. The cumulative distribution of σ_H (calculated over the range $[0.75−3]$ Mpc) is presented in Fig. 4. The plot shows that more than half the LG-like objects in both models have a $\sigma_H \leqslant 60$ km/s. So, many objects have a flow as cold, or colder, as the actual LG. Yet, as was pointed by Macciò et al. (2005) the real problem of the coldness lies with the relation between σ_H and the mean density around the objects.

It follows that the local Hubble flow around ΛCDM and OCDM LG-like objects is essentially indistinguishable. This stands in clear contradiction with previous claims of Baryshev et al. (2001), Chernin et al. (2007c) and Chernin et al. (2007a). Also, both the ΛCDM and OCDM LG-like groups obey equally well the escape velocity prediction of the flat -Λ cosmology, as if they are not affected by the Λ term.

5 THE LOCAL GRAVITATIONAL FIELD

To understand the possible reason for the discrepancies between the present results and the and the model predictions we have studied the nature of the local gravitational field. The prime motivation here is to check the validity of the

Chernin et al. (2007c) model of the gravitational field (Eq. 1), which corresponds to the full gravitational field expressed in physical, and not co-moving, coordinates. The relation between the peculiar gravity (output of GADGET) and the physical one was derived by Martinez-Vaquero et al. (2007), but it is repeated here for the sake of completeness.

The physical $\mathbf{r}$ and comoving $\mathbf{x}$ coordinates are related by: $\mathbf{r} = a\mathbf{x}$. The gravitational field equals the physical acceleration of an object $\ddot{\mathbf{r}} = \mathbf{g}$. The GADGET code provides an acceleration-like term defined as:

$$\mathbf{f}_p = \frac{1}{a}\frac{d}{dt}\left(a \cdot \mathbf{v}_p\right) = \dot{\mathbf{v}}_p + H \cdot \mathbf{v}_p, \tag{2}$$

where $\mathbf{v}_p = \dot{\mathbf{r}} - H\mathbf{r}$ is the peculiar velocity, H is Hubble's constant and a is the expansion scale factor. It follows that

$$\ddot{\mathbf{r}} = \mathbf{f}_p + \mathbf{r}\frac{\ddot{a}}{a} = \mathbf{f}_p + \left(-\frac{1}{2}\Omega_M + \Omega_\Lambda\right)H^2\mathbf{r}. \tag{3}$$

Namely, the linear term corresponds to the unperturbed Friedman solution and $\mathbf{f}_p$ to the fluctuating component[1].

The gravitational field is taken with respect to the LG reference frame. So that, one finally obtain:

$$g = \left(\mathbf{f}_p - \mathbf{f}_p^{LG}\right)\frac{\mathbf{r}}{r} + \left(-\frac{1}{2}\Omega_M + \Omega_\Lambda\right)H^2 r \tag{4}$$

where r is the distance from the center of mass of the LG. This is the field acting on each dark matter particle. The total acceleration of halos was computed by averaging this quantity over all particles belonging to each halo. The acceleration is scaled by $H_0^2 \times 1$ Mpc. In such scaling the unperturbed gravitational acceleration of a shell of radius 1 Mpc equals to $-q_0$, where q_0 is the cosmological deceleration parameter.

In Figs. 5 and 6 we compare the radial component of the exact (*i.e.* in the sense of the simulations) gravitational field with the Chernin et al. (2007c) model (g_{PP}), as traced by the DM halos around the LG-like objects. Only the fluctuating component of the gravitational field is shown in the figures, namely for the numerically exact field it is the radial component of $\mathbf{f}_p$ and for the point particle approximation it is $f_{p,PP} = -GM_{LG}/r^2 + \Omega_M H^2 r/2$. We show all DM halos in the distance range of $0.7 \leqslant r \leqslant 3.0$ Mpc from the same LG-like objects that were presented in Figs. 1 and 2. Since DM halos closer that $r = 0.7$ Mpc are affected by the two-body dynamics of the LG, they are excluded here. Fig. 7 shows the scatter plot of the gravitation field of all the LG-like objects of the ΛCDM and OCDM simulations. The plots show that the numerically exact value of the radial component of $\mathbf{f}_p$ and the point particle prediction ($f_{p,PP}$) are very poorly correlated. A linear regression analysis finds a correlation coefficient of 0.40 (0.23) and a slope of 0.35 (0.16) for the ΛCDM (OCDM) model. It is clear that the point particle model fails to reproduce the actual gravity field, and therefore it cannot account for the dynamics of the LG.

---

[1] Note the typo in Eq. A3 of Martinez-Vaquero et al. (2007) where Ω_Λ was omitted. However, this did not affect the result, as only the fluctuating term of g was considered there.

6 DISCUSSION

The most striking result of this paper is that the local Hubble flow around LG-like objects in the OCDM model is almost indistinguishable from the ΛCDM flow. To the extent that the models do differ it is the OCDM model that has somewhat colder Hubble flow than the ΛCDM one. It follows that the local flow is not affected by the DE and does not manifest the present epoch dominance of the DE.

One should not be surprised by the departure of the simulated local Hubble flow from the prediction of the simple model proposed by Chernin et al. (2007c). First, the actual gravitational field deviates considerably from the predicted one. Second, the gravitational dynamics is not local and the tidal field plays an important role in the quasi-linear regime (Hoffman 1986, Hoffman 1989, Zaroubi & Hoffman 1993, van de Weygaert & Babul 1994, Del Popolo et al. 2001). It follows that the dynamics depends not only on the local field, but is also affected by the shear, namely the tidal field. The shear breaks the simple linear relation of the density and velocity fields of the linear regime and therefore the local density field cannot account for the local Hubble flow.

The comparison of the ΛCDM and OCDM simulations shows that they yield very similar LG-like objects with virtually identical local Hubble flows. It follows that the dynamical properties of LG-like objects and their environments, in the linear and quasi-linear regime, depend mostly on the cold matter content of the universe, namely Ω_m, and only weakly on the DE. This is another manifestation of the fact that the properties of the cosmic web, expressed in co-moving coordinates, depend mostly on Ω_m and hardly on the DE (Hoffman et al. 2007).

APPENDIX

Assuming the local gravitational field around the LG is indeed given by the point particle approximation (Eq. 1), the effective Newtonian potential is given by

$$\phi(r) = -\frac{GM_{LG}}{r} - \frac{\Omega_\Lambda H_0^2 r^2}{2}. \tag{5}$$

The effective Newtonian energy (per unit mass) is simply given as $\epsilon = v^2/2 + \phi(r)$. In the presence of the Λ term the potential reaches a maximum at R_V at which the potential peaks at $\epsilon_V \equiv \phi(R_V)$. It follows that a particle is unbound to the LG if its energy is larger than ϵ_V. The escape velocity is therefore given by

$$\frac{v_{esc}^2}{2} = GM_{LG}\left(\frac{1}{r} - \frac{1}{R_V}\right) + \frac{\Omega_\Lambda H_0^2}{2}\left(r^2 - R_V^2\right). \tag{6}$$

In the case of a vanishing cosmological constant the classical expression of Eq. 5 and 6 is recovered upon substituting $R_V = \infty$ and $\Omega_\Lambda = 0$. It should be reemphasised here that the present derivation is done under the assumption of the point particle approximation. The analysis of the simulation proves that the assumption is inapplicable to the LG systems.

REFERENCES

Baryshev, Y. V., Chernin, A. D., & Teerikorpi, P. 2001, A&A, 378, 729

Chernin, A. D., Karachentsev, D. I., Kashibadze, I. D., Makarov, O. G., Teerikorpi, P., Valtonen, M. J., Dolgachev, V. P., & Domozhilova, L. M. 2007a, ArXiv e-prints, 0706.4171

Chernin, A. D., Karachentsev, I. D., Teerikorpi, P., Valtonen, M. J., Byrd, G. G., Efremov, Y. N., Dolgachev, V. P., Domozhilova, L. M., Makarov, D. I., & Baryshev, Y. V. 2007b, ArXiv e-prints, 0706.4068

Chernin, A. D., Karachentsev, I. D., Valtonen, M. J., Dolgachev, V. P., Domozhilova, L. M., & Makarov, D. I. 2004, A&A, 415, 19

—. 2007c, A&A, 467, 933

Chernin, A. D., Teerikorpi, P., & Baryshev, Y. V. 2006, ArXiv Astrophysics e-prints, 0603226

Del Popolo, A., Ercan, E. N., & Xia, Z. 2001, AJ, 122, 487

Gill S. P. D., Knebe A., Gibson B. K., 2004, MNRAS, 351, 399

Hoffman, Y. 1986, ApJ, 308, 493

—. 1989, ApJ, 340, 69

Hoffman, Y., Lahav, O., Yepes, G., & Dover, Y. 2007, JCAP, 10, 16

Hoffman, Y. & Ribak, E. 1991, ApJ, 380, L5

Karachentsev, I. D. 2005, AJ, 129, 178

Karachentsev, I. D., Karachentseva, V, Huchtmeier, W, Makarov, D., Kaisin, S., & Sharina, M. 2007, arXiv:0710.0520

Klypin, A., Gottlöber, S., Kravtsov, A. V., & Khokhlov, A. M. 1999, ApJ, 516, 530

Klypin, A., Hoffman, Y., Kravtsov, A. V., & Gottlöber, S. 2003, ApJ, 596, 19

Kravtsov, A. V., Klypin, A., & Hoffman, Y. 2002, ApJ, 571, 563

Lahav, O., Lilje, P. B., Primack, J. R., & Rees, M. J. 1991, MNRAS, 251, 128

Macciò, A. V., Governato, F., & Horellou, C. 2005, MNRAS, 359, 941

Martinez-Vaquero, L. A., Yepes, G., & Hoffman, Y. 2007, MNRAS, 378, 1601

Reiprich, T. H. & Böhringer, H. 2002, ApJ, 567, 716

Springel, V. 2005, MNRAS, 364, 1105

Teerikorpi, P., Chernin, A. D., & Baryshev, Y. V. 2005, A&A, 440, 791

Tonry, J. L., Dressler, A., Blakeslee, J. P., Ajhar, E. A., Fletcher, A. B., Luppino, G. A., Metzger, M. R., & Moore, C. B. 2001, ApJ, 546, 681

van de Weygaert, R. & Babul, A. 1994, ApJ, 425, L59

Willick, J. A., Courteau, S., Faber, S. M., Burstein, D., Dekel, A., & Strauss, M. A. 1997, ApJS, 109, 333

Zaroubi, S. & Hoffman, Y. 1993, ApJ, 414, 20

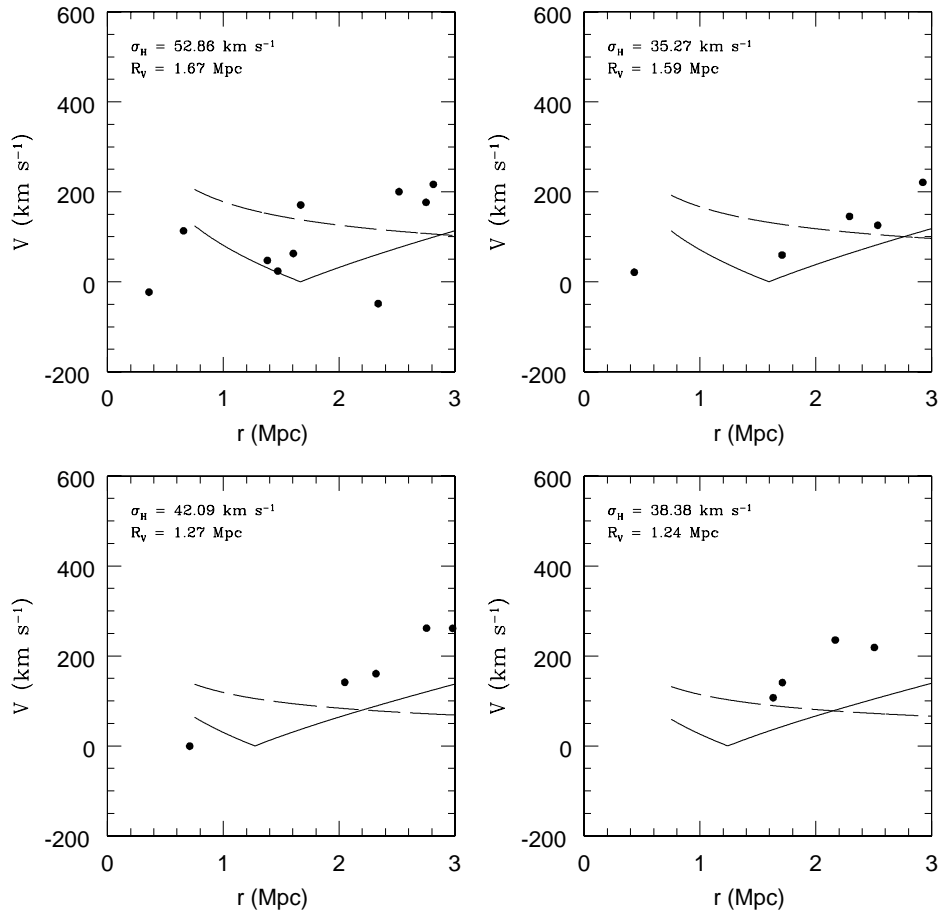**Figure 1.** The Hubble diagrams around four LG-like objects in the ΛCDM simulation. The scatter plots represent the radial peculiar velocity of the DM halos *vs.* the distance from the MW and M31-like DM halos. The solid curve corresponds to the escape velocity profile of the ΛCDM model, calculated under the assumption of the point particle approximation. For reference the escape velocity of the corresponding OCDM model is given as well (dashed line), namely it is calculated as if the Λ term is missing. The value of σ_H, taken over the range $0.75 \leqslant r \leqslant 3$ Mpc and R_V of each object is given.
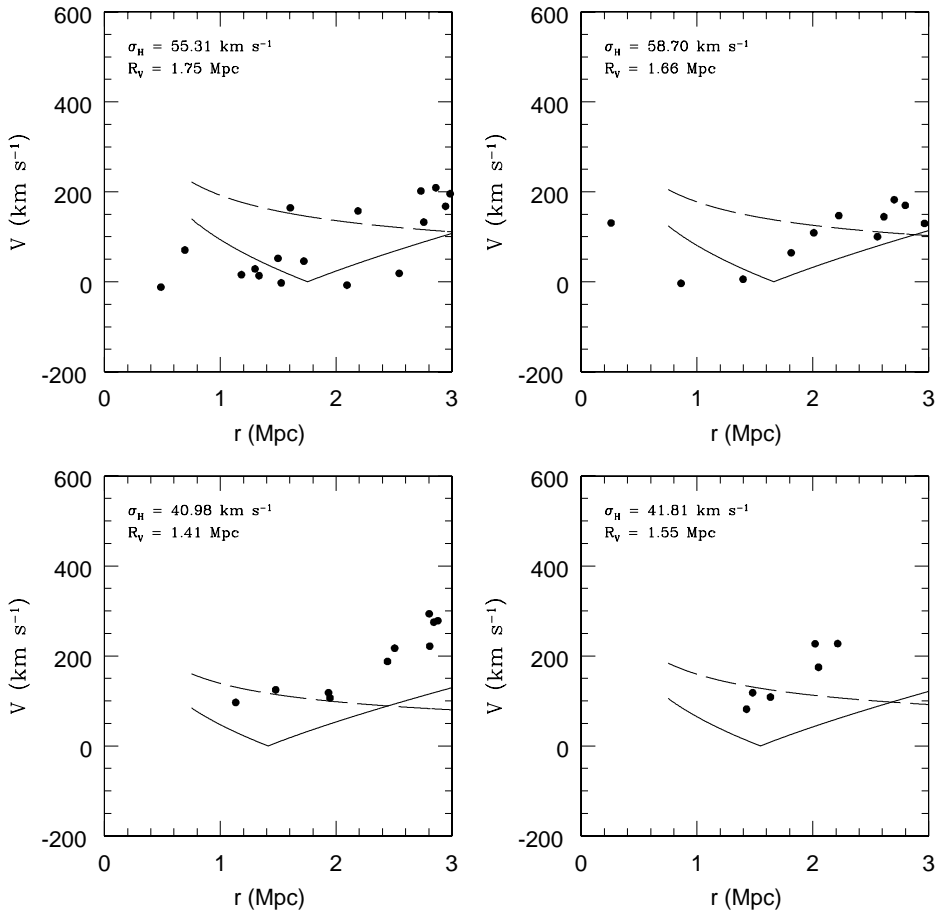
Figure 2. The Hubble diagrams around four LG-like objects in the OCDM simulation. The four LG-like objects shown here are the OCDM counterparts of the ΛCDM ones shown in Fig. 1. The structure and notations of the plots are the same as in Fig. 1.
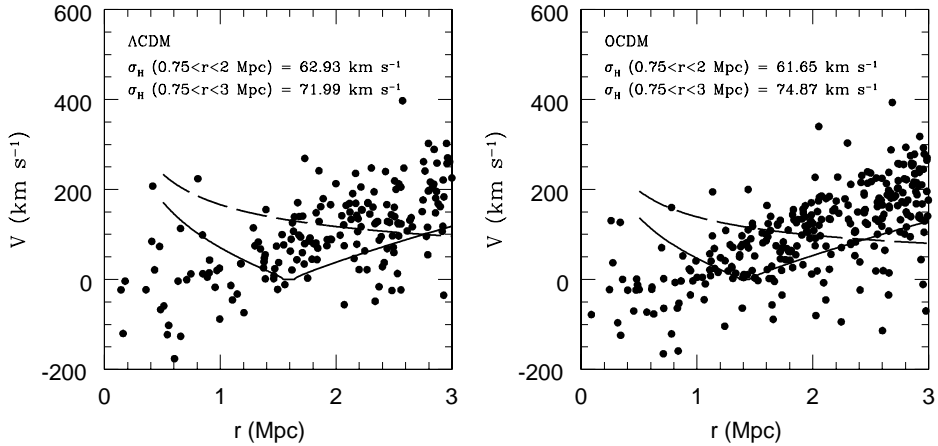

Figure 3. Combined Hubble diagram of 26 LG candidates in the ΛCDM (left panel) and 43 candidates in the OCDM (right panel) models. The radial distance r is scaled by the value of R_V of each object. The values of σ_H within 2 and 3 Mpc are given in Table 1. The escape velocity curves are plotted in the same manner as in Figs. 1 and 2. $< R_V >$ is the mean R_V of all the LG-like objects for each simulation.

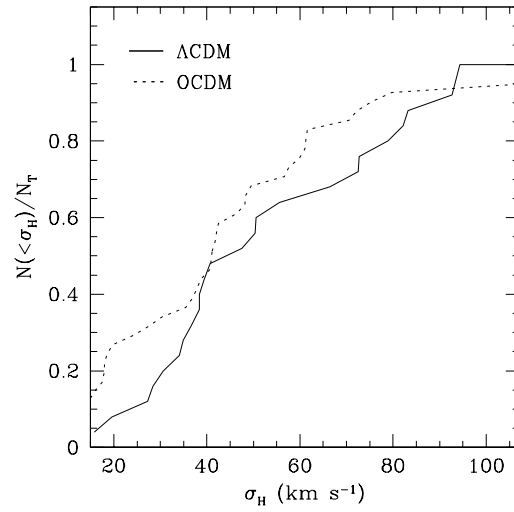**Figure 4.** The fractional cumulative σ_H function of LG-like objects, namely the fraction of objects with σ_H lower than a certain value. Full line corresponds to the 26 ΛCDM objects and the dashed one to the 43 OCDM objects. The dispersion around a pure Hubble flow, σ_H, is calculated over the range $0.75 \leqslant r \leqslant 3$ Mpc.
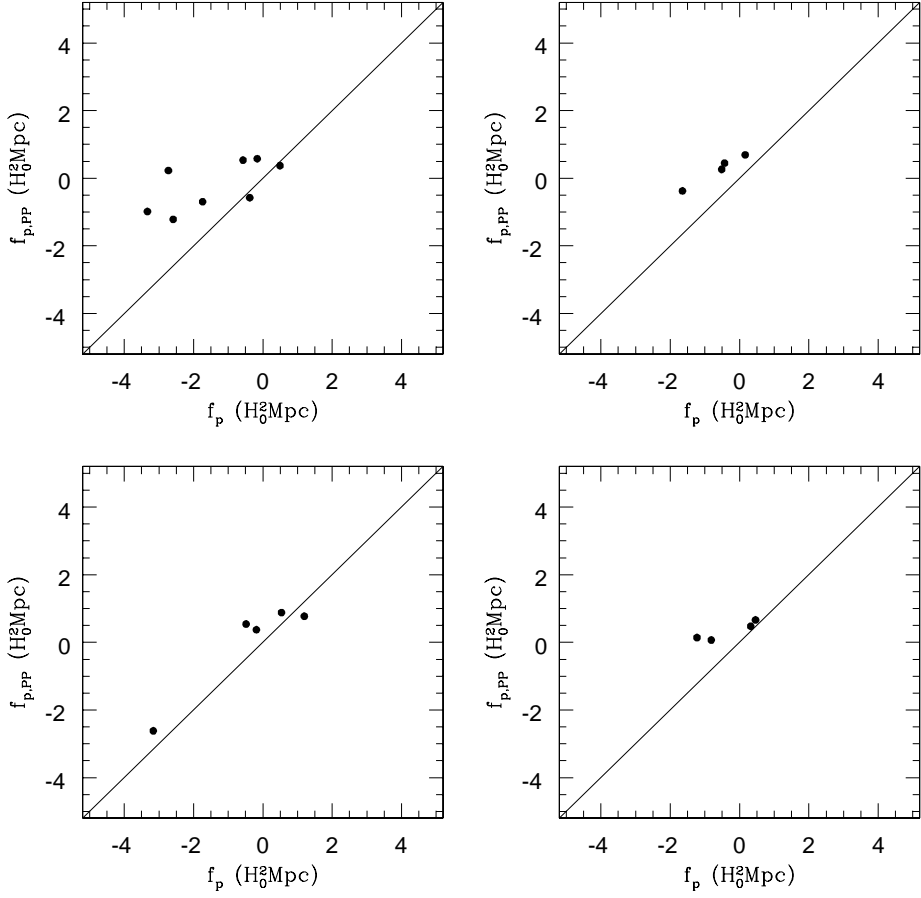
Figure 5. The ΛCDM gravitational field: A scatter plot of the exact gravitational field g (Eq. 4) *vs.* the approximated one g_{PP} (Eq. 1) experienced by DM halos around LG-like objects. The four objects and panels correspond to the ones in Fig. 1. Only DM halos in the range of $0.75 \leqslant r \leqslant 3.0$ Mpc are plotted here. The gravitational field is scaled by $H_0^2 \times 1$ Mpc.
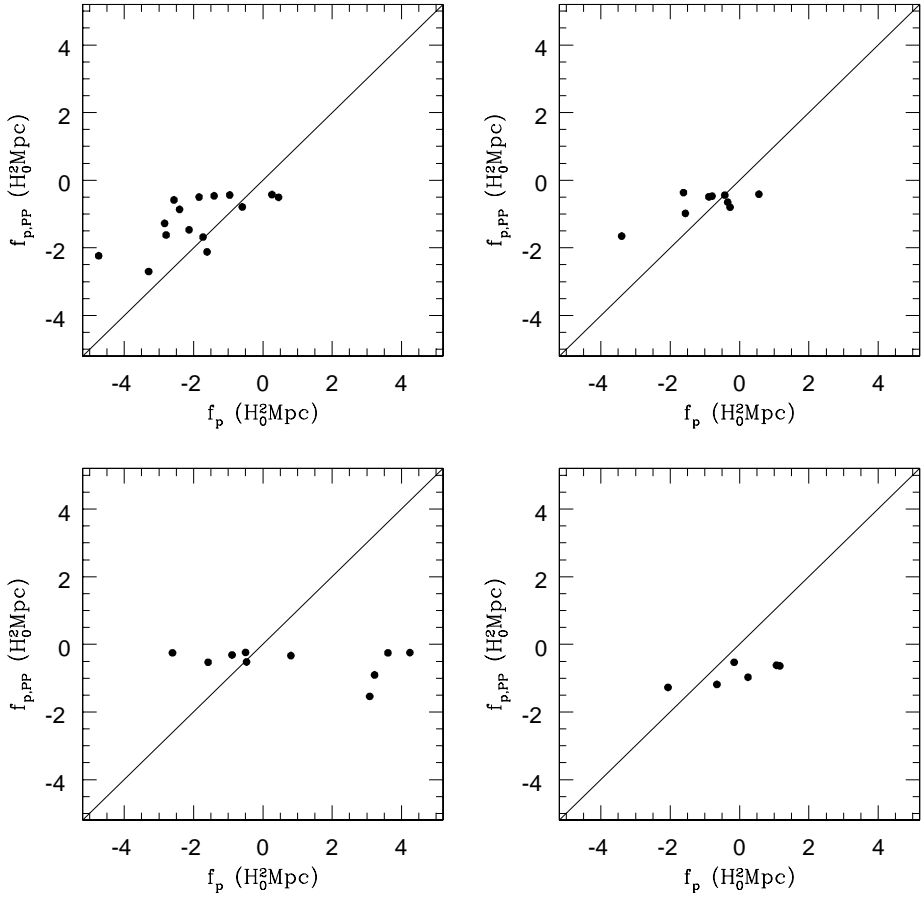
Figure 6. Same as Fig. 5 but for the OCDM simulation. The LG-like objects and panels correspond to the ones in Fig. 2.
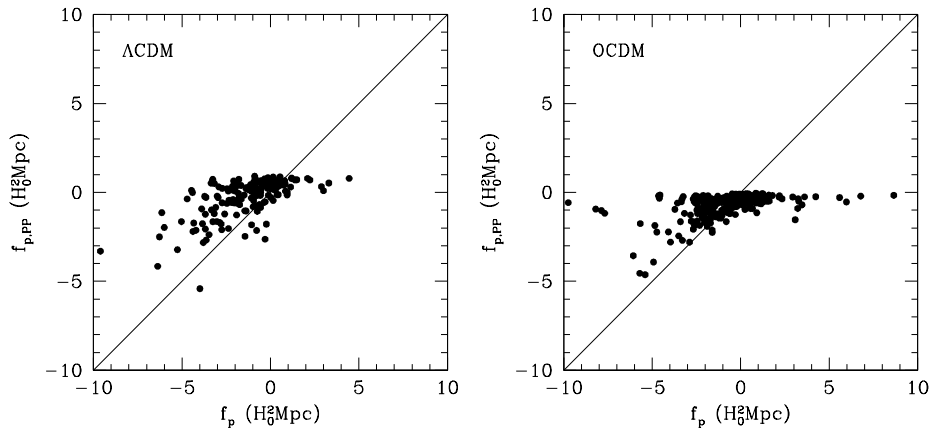

Figure 7. Scatter plot of the fluctuating component of the gravitational field predicted by the point particle model $(f_{p,PP})$ against the exact value calculated by the simulations. The left panel shows the distribution of the DM halos in the vicinity $(0.75 \leqslant r \leqslant 3.0$ Mpc$)$ of the 26 LG-like ΛCDM objects and the right panel exhibits the 43 OCDM objects. The gravitational field is scaled by $H_0^2 \times 1$ Mpc.